Structural Engineering and Mechanics, Vol. 37, No. 5 (2011) 509-527
DOI: http://dx.doi.org/10.12989/sem.2011.37.5.509

Dynamic buckling analysis of a composite stiffened cylindrical shell

S.N. Patel[1a], C. Bisagni*[1] and P.K. Datta[2b]

[1]*Department of Aerospace Engineering, Politecnico di Milano, Milano, Italy*
[2]*Department of Aerospace Engineering, Indian Institute of Technology, Kharagpur, India*

(Received December 22, 2009, Accepted November 10, 2010)

Abstract. The paper investigates the dynamic buckling behaviour of a laminated composite stiffened cylindrical shell using the commercial finite element code ABAQUS. The numerical model of the composite shell is validated by static tests. In particular, the experimental collapse test is numerically simulated by a quasi static analysis carried out by both ABAQUS/Standard and ABAQUS/Explicit. The behaviour in the post-buckling field and the collapse load obtained by the analyses are close to the experimental data. The validated model is then used to study the dynamic buckling behaviour with ABAQUS/Explicit. The effects of the loading magnitude and of the loading duration are investigated, implementing in the analysis also first-ply failure criteria. It is observed that the dynamic buckling load is highly affected by the loading duration.

Keywords: dynamic buckling; composite stiffened shell; pulse loading; failure; finite element analysis.

1. Introduction

The dynamic buckling phenomenon of thin-walled stiffened structures has drawn considerable attention of many scientists, researchers and designers in the last few decades due to its importance for the aircraft and space industries. The stiffened cylindrical shells are important structural components in the aircraft and missile industries, and, in the recent years, the composite materials have been increasingly used for making these structural components more efficient thank to their high stiffness-to-weight ratio and high strength-to-weight ratio, but also because they can be tailored through the variation of fibre orientation and stacking sequence. So there is a vast interest for further investigation on the dynamic buckling behaviour of these structures, as they can be subjected to dynamic loads for short duration in cases like aircraft landing, take-off and manoeuvring.

Under dynamic loading environments, two different classes of structural phenomena are usually identified: parametric excitation and dynamic buckling (Jansen 2005). The parametric excitation is a vibration buckling phenomenon under the action of pulsating loading condition, while the dynamic buckling is defined as the behaviour of a structure which is subjected to step loading or impulsive

*Corresponding author, Associate Professor, E-mail: chiara.bisagni@polimi.it
[a]Former Post-Doctoral Fellow, E-mail: shuvendu_patel@yahoo.co.in
[b]Professor, E-mail: pkdatta@aero.iitkgp.ernet.in

loading, that leads to stability loss. According to Kubiak (2007), the dynamic buckling occurs when the loading process is of intermediate amplitude, and the pulse duration is close to the period of fundamental natural flexural vibrations, that are in the range of milliseconds. Budiansky and Roth (1962) studied, in the 60's, the axisymmetric dynamic buckling of clamped shallow spherical shells and calculated the deformation of the shell due to a transient pressure loading. They also suggested a criterion for dynamic buckling as a function of loading duration. Lindberg and Florence (1987) have published the monograph summarizing the results from research on dynamic buckling of metallic structures like bars, plates, rings and shells under different types of pulse loading. The work mainly describes the effect of high amplitude short duration load in all problems they have taken. They classify this buckling as high-order dynamic buckling. In most of the problems the amplitude is much higher than the static buckling load. However, the published work emphasizes the importance of low-order dynamic buckling i.e., buckling with low amplitude higher duration dynamic load in conventional structural design including the fundamentals of low-order dynamic buckling of column alone. Moreover, they have also reported that the spherical cap, arches and cylindrical shells are extremely sensitive to initial imperfections in low-order dynamic buckling. As a result the critical dynamic buckling loads of long duration (e.g., step load) can be smaller in magnitude then the corresponding static buckling load. More recently, Simitses (1990) studied extensively the dynamic stability behaviour of suddenly loaded structures, while Karagiozova and Jones (1996) analyzed the dynamic elastic-plastic buckling phenomenon using a multi-degrees-of-freedom model, which retains the influences of axial and lateral inertia and the effects of initial geometrical imperfections.

Several investigations were performed in the last 10 years using finite element methods. Yaffe and Abramovich (2003) used the finite element code ADINA to investigate the buckling behaviour of aluminium stringer stiffened shells under axial dynamic loading. They showed numerically that the shape of the loading period, as well as the initial geometric imperfections had a great influence on the dynamic buckling of the shells. They also conducted some experiments to cause a shell to buckle dynamically. Using finite element analyses, Bisagni and Linde (2006) studied the structural behaviour of ortothropically stiffened aluminium aircraft panels subjected to dynamic loading. Focus was placed on a stringer-frame stiffened circular aircraft fuselage panel loaded by different duration load pulses.

Few publications can be found in the literature regarding the dynamic buckling aspects of composite structures. Papazoglou and Tsouvalis (1995) developed an analytical solution method for the dynamic buckling behaviour of a laminated plate subjected to time-dependent uniformly distributed normal and shear in-plane loads. Huyan and Simitses (1997) studied the dynamic stability of circular metallic and laminated cylindrical shells. The cylinders were geometrically imperfect and subjected to axial compression or pure bending moment. These loads were suddenly applied with constant magnitude and finite or infinite duration.

Ari-Gur and Simonetta (1997) carried out the investigation on dynamic pulse buckling of rectangular composite plates through an explicit finite-difference integration scheme. The applied load was either a force or displacement pulse, and the buckling loads were determined for various loading durations and material lay-up configurations. Gupta *et al.* (2003) investigated the nonlinear asymmetric dynamic buckling of clamped laminated angle-ply composite spherical caps under suddenly applied pressure loads. Their formulation was based on first-order shear deformation theory, and they obtained the buckling load through dynamic response history using Newmark's integration scheme coupled with Newton-Raphson iteration scheme.

Sofiyev (2005) studied the buckling of orthotropic cylindrical thin shells with material non-

homogeneity in the thickness direction under impulsive torsion loading; while Liu *et al.* (2005) combined the finite element method with two different stability criteria, namely the Budiansky and the phase-plane buckling criteria to study the dynamic buckling phenomena of plate and shell structures subjected to sudden applied loading.

Kolakowski and Kubiak (2007) analyzed the dynamic response of a thin-walled laminated column subjected to in-plane pulse loading taking into account the shear lag phenomenon and the distortional deformations. The problem of nonlinear stability was solved with the transition matrix method.

Petry and Fahlbush (2000) investigated the dynamic stability behaviour of imperfect simply supported plates subjected to in-plane pulse loading. The large-deflection plate equations were solved by a Galerkin method using Navier's double Fourier series. For the calculation of dynamic buckling loads a stress failure criterion was applied. Parametric studies were performed in which the influences of pulse duration, shock function, imperfection, geometric dimensions and limit stress of the material were discussed.

Bisagni (2005) reported the results of the dynamic buckling due to impulsive loading of thin-walled carbon fiber reinforced plastics shell structures under axial compression. The approach adopted was based on the equations of motion, which were numerically solved using the finite element code ABAQUS/Explicit. It was shown numerically that the initial geometric imperfections as well as the duration of the loading period had a great influence on the dynamic buckling of the shells.

Recently Kubiak (2007) proposed a criterion of dynamic buckling of thin walled structures. He analyzed the local, global and interactive dynamic buckling of plates and beam-columns made of isotropic or orthotropic material with open cross-sections subjected to compressive rectangular pulse loading.

Abramovich and Grunwald (1995) conducted an experimental series on laminated composite plates, and studied the dynamic stability behaviour of the plates. The experimental studies with axially impacted laminated composite plates having various aspect ratios and boundary conditions were performed to determine the dynamic load amplification factor. The static and dynamic buckling loads were determined using a modified Donnell approach to yield consistent results.

Bisagni (2004) experimentally investigated the elastic dynamic buckling of carbon fiber reinforced plastic cylindrical shells subjected to pulse axial compression. The critical impulse was applied using a horizontal crash sled, so to obtain axial compression shape similar to a half-sine and duration of the impact load of approximately 0.1 s. The dynamic buckling load of the initially imperfect shell was related to its static buckling load.

The present investigation numerically finds the dynamic buckling characteristics of a laminated composite stiffened shell subjected to axial impulsive impact loading.

The study is performed using the commercial finite element codes ABAQUS/Standard and ABAQUS/Explicit, and reports also the first ply failure indices together with the dynamic buckling results. Moreover an adaptation of the Volmir criterion (Volmir 1972, Kubiak 2007) is used to define the dynamic buckling load of the stiffened structure.

2. Composite stiffened cylindrical shell

The investigated composite stiffened cylindrical shell is made of carbon fibre reinforced plastic

(CFRP) fabric material laid up on a mandrel and cured in an autoclave (Bisagni and Cordisco 2004). The ply material properties are reported in Table 1.

The shell is characterized by an inner radius of 350 mm. The overall length is equal to 700 mm, but it includes two tabs at the top and at the bottom surfaces for fixing the shell into the test facility, so that the actual length of the cylinder is equal to 540 mm.

The skin is made of two plies oriented at [45°/–45°], where zero degree is the axial direction of the shell, and the numbering of the plies starts from the inner side.

Eight L-shaped stringers are bonded and riveted to the skin. They are internally located and equally spaced in the circumferential direction. The blade of the stiffeners is 25 mm long, while the flange attached to the skin is 32 mm long. The stringers consist of 12 plies oriented at $[0°/90°]_{3s}$.

In correspondence of the stringers, on the outer side of the shell, three plies of reinforcement are added with [0°/45°/–45°] orientation. The reinforcement is 40 mm width and is long as the shell.

A photo of the composite stiffened cylindrical shell is reported in Fig. 1, together with the finite element model for ABAQUS. In the model the circumferential to longitudinal divisions of the cylinder skin is 320 × 80, and the whole model consists of 39680 S4R shell elements. A detail of one of the stiffened portions is shown in Fig. 2. The dimensions of the elements are 4 × 6.75 mm for the reinforcement, the skin under the reinforcement and the stiffener flange, 6.25 × 6.75 mm for the stiffener blade and 7.83 × 6.75 mm for the other parts of the skin.

All six boundary conditions are restrained in the bottom surface of the shell, while in the top surface the axial displacement is allowed keeping restrained the other five boundary conditions.

Table 1 Mechanical properties of CFRP ply

Elastic modulus E_{11} (N/mm^2)	Elastic modulus E_{22} (N/mm^2)	Shear modulus G_{12} (N/mm^2)	Poisson's ratio ν_{12}	Density (kg/m^3)	Thickness (mm)
57765	53686	3065	0.048	1510	0.33

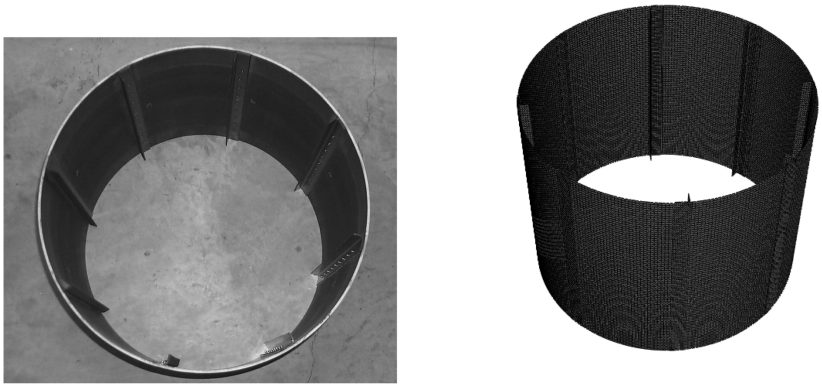

(a) (b)

Fig. 1 Composite stiffened shell (a) specimen, (b) numerical model for ABAQUS

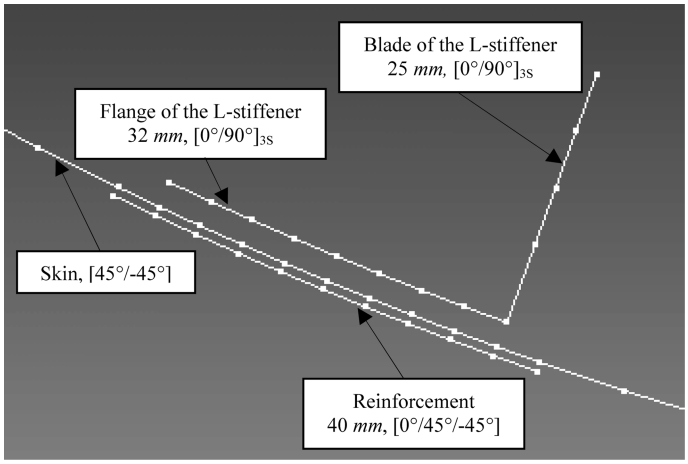

Fig. 2 A stiffened portion of the shell in the numerical model

3. Simulation of the static test

At first, an eigenvalue buckling analysis of the laminated composite stiffened shell is carried out using ABAQUS/Standard. Then, the collapse test performed under compression with displacement control is simulated as a slow dynamic analysis using both ABAQUS/Standard and ABAQUS/Explicit.

3.1 Eigenvalue buckling analysis

The eigenvalue buckling analysis of the laminated composite stiffened cylinder is carried out using ABAQUS/Standard.

The buckling load obtained by the analysis results equal to 242 kN. The buckling modes is shown in Fig. 3 with a deformation scale factor of 12.

Fig. 3 Buckling shape of the stiffened cylindrical shell

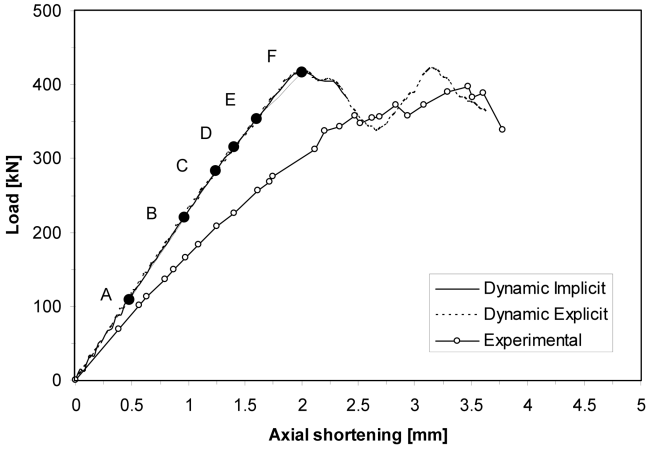

Fig. 4 Comparison between numerical and experimental load-shortening curves

Table 2 Numerical and experimental collapse loads

Method of analysis	Collapse load (kN)	Percentage difference
ABAQUS/Standard: dynamic analysis	416.83	+4.8%
ABAQUS/Explicit: dynamic analysis	419.40	+5.4%
Experimental test (Bisagni and Cordisco 2004)	396.70	-

3.2 Collapse analysis

A non-linear collapse analysis of the laminated composite stiffened cylindrical shell is carried out by a slow dynamic analysis to simulate the static compression test performed experimentally with displacement control. The equations of equilibrium governing the dynamic response of the stiffened shell are solved by both explicit integration operator (ABAQUS/Explicit) and implicit integration operator (ABAQUS/Standard). Both methods are so used to study the buckling and post-buckling behaviour of the stiffened cylinder until the collapse. In particular, in the analysis, a uniform displacement is applied on the shell top surface with the rate of 8 mm per second, and the reaction forces in all nodes are summed to trace the load-shortening curve.

The load-shortening curves obtained by both types of dynamic analyses are plotted in Fig. 4 along with the experimental curve. The values of the collapse load obtained by the two numerical analyses are compared to the experimental data in Table 2.

The difference between the numerical and experimental collapse load is around 5 percent. The difference between the shortening in correspondence of the collapse is a little higher, as the numerical model is not able to take correctly the real stiffness of the shell. This may be due to the formulation of the FEM code used by ABAQUS. FEM code is based on the Energy Methods which always gives the upper bound because of the over-stiffness due to approximate shape functions which are truncated. Also the energy due to membrane stretching of the shell panel is significant. Theoretical static buckling load will also be higher compared to the experimental one and there will

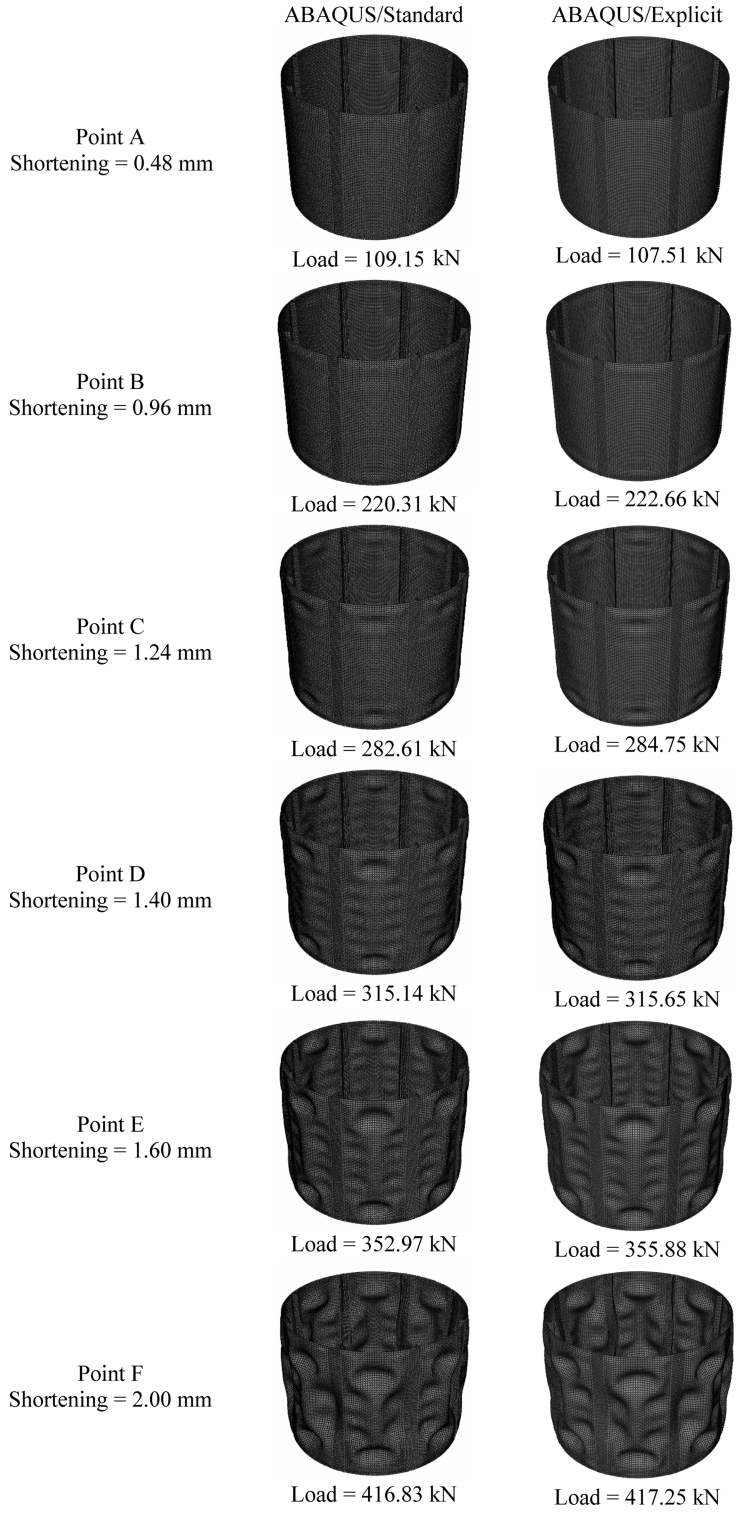

Fig. 5 Evolution of shell deformation shape during the collapse analysis

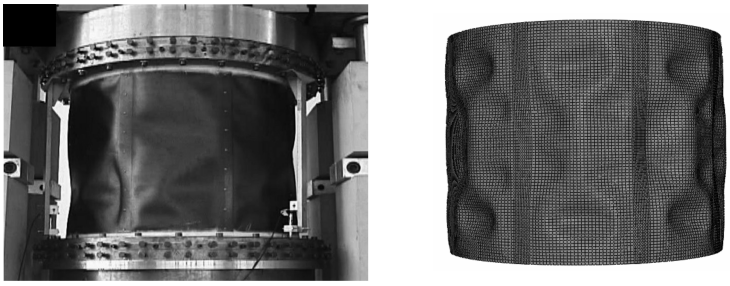

(a) (b)

Fig. 6 Post-buckling shapes (a) experimental test, (b) ABAQUS/Explicit analysis

Table 3 CPU time for the dynamic analyses

Type of analysis	CPU time (Minutes)
ABAQUS/Standard: dynamic analysis	91
ABAQUS/Explicit: dynamic analysis	52

be some over estimate of the dynamic buckling load also. However, the FEM modelling has made good estimate of the collapse load. Indeed, the finite element model was kept as much as simple as possible and was considered acceptable if able to capture the values of the collapse load.

The collapse load results about 1.7 times higher than the buckling load, obtained by the eigenvalue linear buckling and equal to 242 kN. The shell shows consequently a large post-buckling field before the collapse, as the skin buckles first but the stiffeners are still capable to withstand more load. The deformation of the stiffened shell is shown in Fig. 5 with a scale factor equal to 5. In particular, Fig. 5 presents the deformations obtained by the dynamic analyses using both ABAQUS/Standard and ABAQUS/Explicit together with the axial shortening and loads obtained in correspondence of the points A to F of the load-shortening curve reported in Fig. 4.

The experimental and numerical deformation shapes in the deep post-bucking field are compared in Fig. 6. The numerical post-buckling mode is similar to the experimental one, showing also the buckling of the stiffeners. The deformation in the skin portion is quite prominent although it is regular in all eight portions of the skin in the numerical model.

The results obtained by both implicit and explicit dynamic analyses are almost the same. The main difference is due to the required CPU time. Table 3 compares the CPU time required up to axial shortening equal to 2.72 mm for the dynamic analysis carried out by both ABAQUS/Standard and ABAQUS/Explicit on a ADM Athlon (tm) machine with 64×2 Dual Core Processor 5600+2.81 GHz and 2 BG Ram. It is possible to note that, for this problem, the CPU time required by ABAQUS/Standard is 1.75 times more than the time required by ABAQUS/Explicit.

3.3 Failure investigation

In the simulation of the static collapse test the first-ply failure indices are evaluated according to different failure theories in each time step of the analysis performed using ABAQUS/Explicit. On the load-shortening curve reported in Fig. 7, the points A, B, C and D are pointed out when the

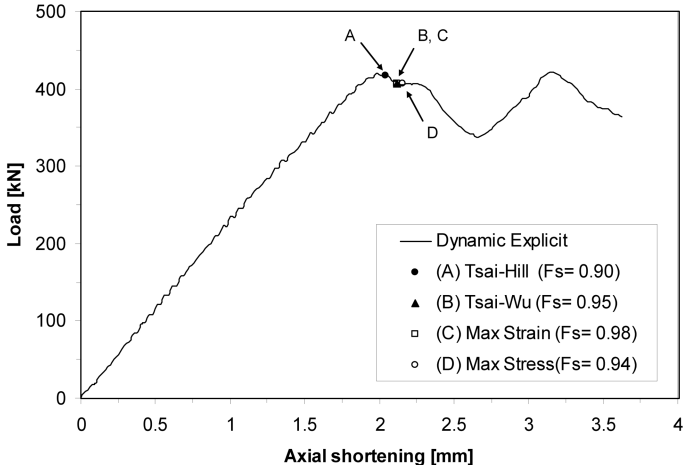

Fig. 7 Load-shortening curve with first-ply failure points

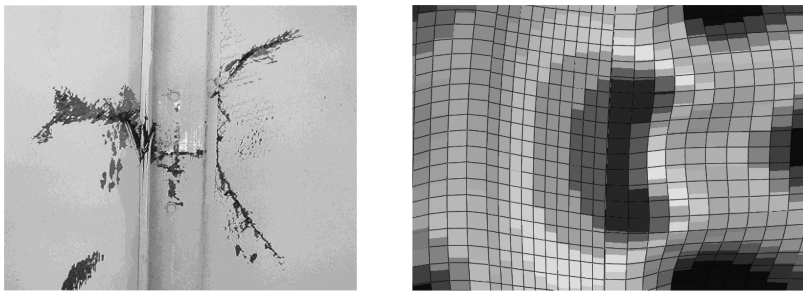

(a) (b)

Fig. 8 Failure (a) experimental test, (b) ABAQUS/Explicit with Maximum Strain theory

failure indices (F_s) are just before 1.0 for Tsai-Hill, Tsai-Wu, Maximum Strain and Maximum Stress failure theories, respectively. It can be observed that the failure indices (F_s) for all failure theories are almost 1.0 at the point when the load is maximum.

The deformation and the failure initiation areas for the different failure criteria are carefully examined, and it is observed that the Maximum Strain criterion is showing the more similar failure pattern to the experimental results, as the failure is initiating in the stiffeners. The experimental and numerical failure modes are shown in Fig. 8.

4. Dynamic buckling analysis

The finite element model validated with the experimental data of the static collapse test is then used to investigate the dynamic buckling behaviour of the laminated composite stiffened cylindrical shell. The dynamic buckling due to the axial load with finite duration is investigated using ABAQUS/Explicit finite element code.

Three different methods are usually considered for the evaluation of the critical conditions for

dynamically loaded elastic systems: total energy phase-plane approach, total potential energy approach and equation of motion approach, often called also Budiansky-Roth criterion (Budiansky and Roth 1962). The equation of motion approach is becoming popular in application, as it can be easily adapted to computational methods like finite element codes, and for this reason is used also in the present research. According to the Budiansky-Roth criterion, the equations of motion are solved for various load parameters, such as magnitude and duration, obtaining the system responses. The critical condition is then defined when a large change in response is obtained.

In the present investigation, the analysed stiffened cylindrical shell, as all stiffened structures, does not present a sudden change in the response. After reaching the maximum load value the load-shortening curve is oscillating without giving a sudden change. So the authors have indirectly taken the static buckling load as the reference to define the dynamic buckling load. If the deformations caused by the static buckling load are possible by any combination of magnitude and duration of dynamic load, then that dynamic load is regarded as dynamic buckling load. The criterion proposed by Volmir (1972) is here used. Volmir analysed a thin plate subjected to in-plane compressive loading with different pulse shape, and defined the following criterion (Volmir 1972, Kubiak 2007):

"Dynamic critical load corresponds to the amplitude of pulse load of constant duration at which the maximum plate deflection is equal to some constant value".

To define the dynamic buckling condition, the linear eigenvalue analysis with static buckling load equal to 242 kN is here taken as reference. Then, from the slow dynamic analysis performed in ABAQUS/Explicit to simulate the collapse test, the axial shortening and the maximum radial displacement are determined in correspondence to 242 kN. They result equal to 1.07 mm and 1.26 mm, respectively. These two displacements are highlighted in Figs. 9 and 10, where the load-shortening curve and the shell deformation are reported.

The dynamic analysis is then performed by ABAQUS/Explicit for different magnitudes of load step, equal to 100, 200, 250, 300, 350 and 400 kN. Each load is applied in a single step as shown in Fig. 11 considering different time duration equal to 0.001, 0.005, 0.01, 0.015 and 0.02 seconds.

The dynamic buckling load of the stiffened cylindrical shell is defined when the axial shortening of 1.07 mm and/or the maximum radial displacement of 1.26 mm is reached during the dynamic analysis. Table 4 shows the dynamic buckling results with respect to axial shortening and/or

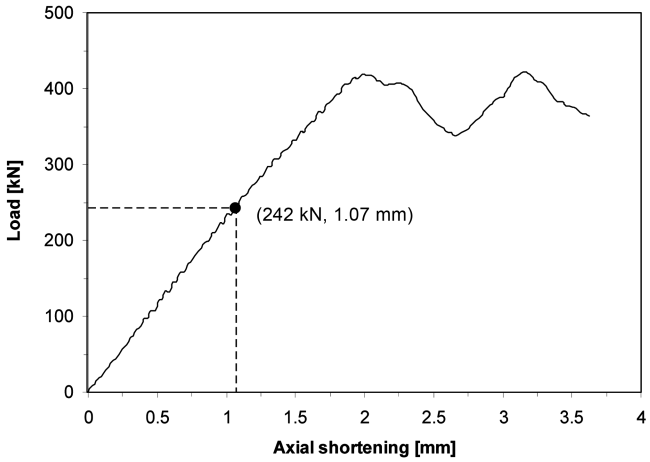

Fig. 9 Quasi static load-shortening curve with highlighted the axial shortening at 242 kN

Fig. 10 Quasi static shell deformation with highlighted the radial displacement at 242 kN

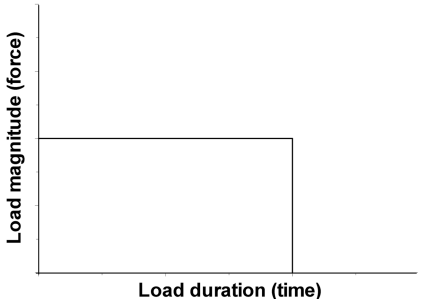

Fig. 11 Loading curve for dynamic buckling

Table 4 Dynamic buckling results

Load (kN)	Displacement	Load step = 0.001 *s*	Load step = 0.005 *s*	Load step = 0.01 *s*	Load step = 0.015 *s*	Load step = 0.02 *s*
100	Axial	Not buckled	Not buckled	Not buckled	Not buckled	Not buckled
	Radial	Not buckled	Not buckled	Not buckled	Not buckled	Buckled
200	Axial	Not buckled	Buckled	Buckled	Buckled	Buckled
	Radial	Not buckled	Not buckled	Buckled	Buckled	Buckled
250	Axial	Not buckled	Buckled	Buckled	Buckled	Buckled
	Radial	Not buckled	Not buckled	Buckled	Buckled	Buckled
300	Axial	Not buckled	Buckled	Buckled	Buckled	Buckled
	Radial	Not buckled	Buckled	Buckled	Buckled	Buckled
350	Axial	Not buckled	Buckled	Buckled	Buckled	Buckled
	Radial	Not buckled	Buckled	Buckled	Buckled	Buckled
400	Axial	Not buckled	Buckled	Buckled	Buckled	Buckled
	Radial	Not buckled	Buckled	Buckled	Buckled	Buckled

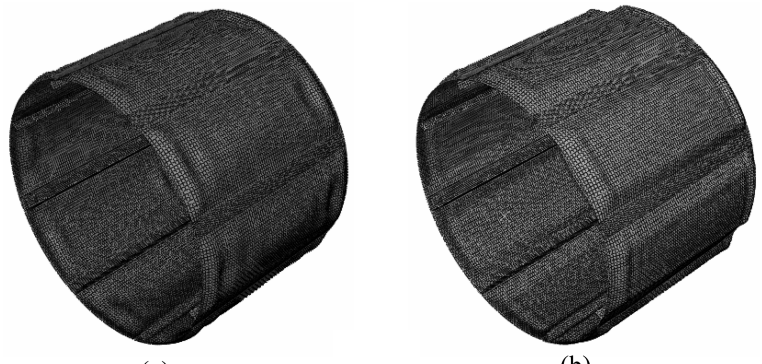

(a) (b)

Fig. 12 Comparison of deformed shapes (a) static buckling, (b) dynamic buckling for load step of 200 kN and duration of 0.01 s

maximum radial displacement for all investigated load steps.

The deformed shape from the quasi static analysis at 242 kN and the dynamic deformed shape for a load step at 200 kN with load duration of 0.01 second are compared in Fig. 12. It is possible to observe that in both deformed shapes the top and bottom portions of the skin between the stiffeners are deformed. Some parts of the skin deformation in the static analysis are inwards, while the deformations are outwards in the dynamic deformed shape.

4.1 Effect of loading duration and magnitude on axial shortening

The effect of loading duration and magnitude on the axial shortening is investigated. The variation of the axial shortening with loading duration and loading magnitude are reported in Figs. 13 and 14, respectively.

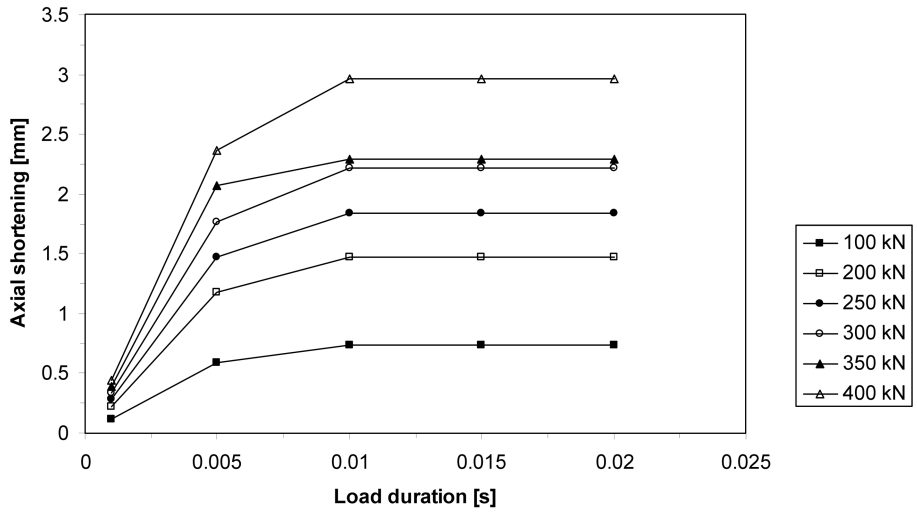

Fig. 13 Variation of axial shortening with load duration for different load magnitudes

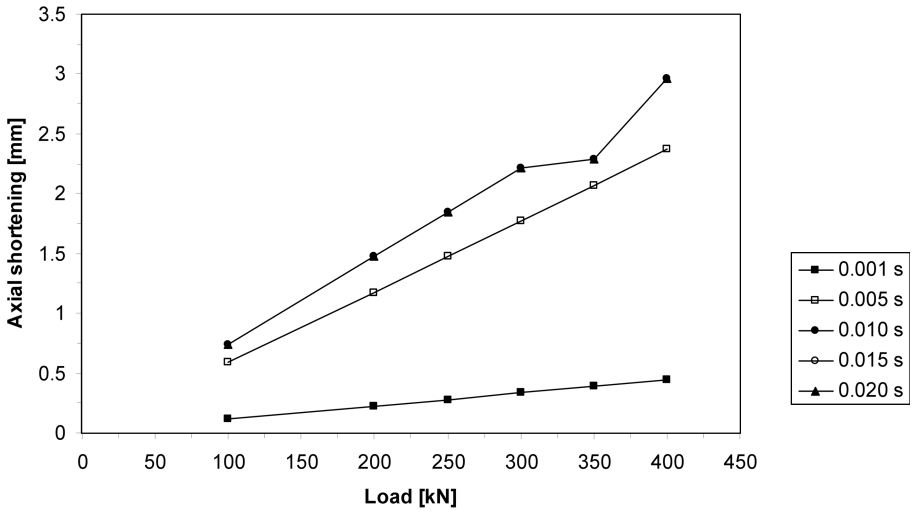

Fig. 14 Variation of axial shortening with load magnitude for different load duration

It is possible to observe that, when the loading duration is increasing, the axial shortening is increasing until a duration equal to 0.01 seconds and then it remains constant. This behaviour is similar for each loading case. On the other hand, when the loading magnitude increases the axial shortening increases gradually. The axial shortening versus load curves for time duration of 0.01, 0.015 and 0.02 seconds coincide one to another.

4.2 Effect of loading duration and magnitude on radial displacement

The effect of loading duration and magnitude on the radial displacement is then investigated. The variation of the maximum radial displacement with loading duration and loading magnitude are

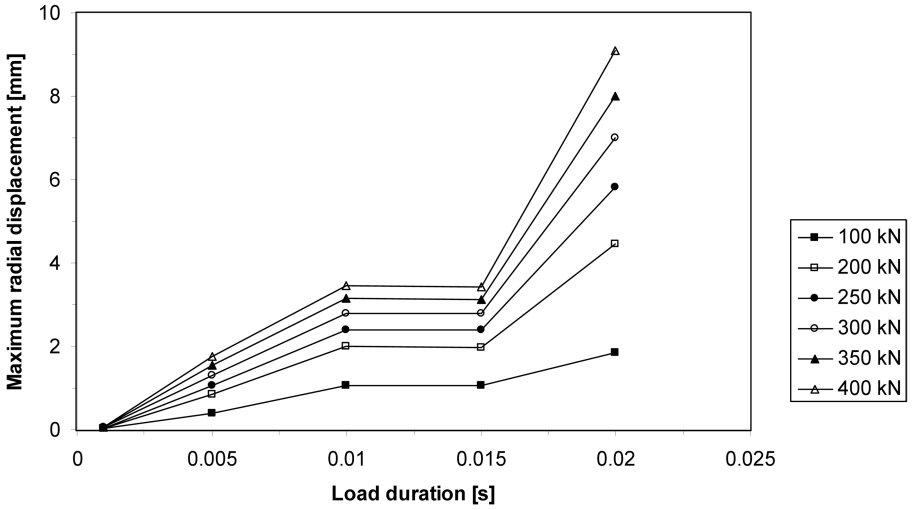

Fig. 15 Variation of radial displacement with load duration for different load magnitudes

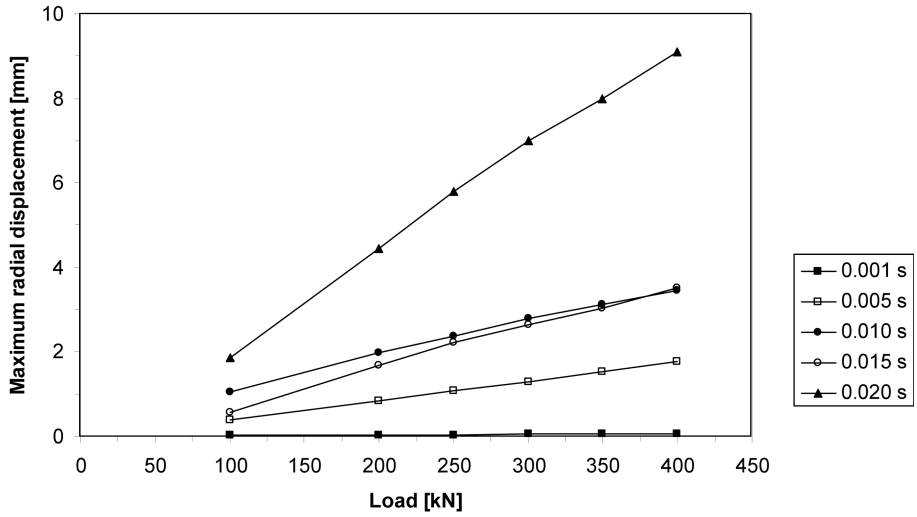

Fig. 16 Variation of radial displacement with loading magnitude for different load duration

reported in Figs. 15 and 16, respectively.

It is possible to observe that, when the loading duration is increasing, the maximum radial displacement is increasing up to the duration of 0.01 seconds. Then, the displacement is almost constant up to 0.015 seconds, and after this point the radial displacement is increasing rapidly for each loading case. On the other hand, the radial displacement is increasing gradually with the increase of load magnitude.

4.3 Effect of loading duration and magnitude on first ply failure

The failure indices are evaluated during each analysis using Maximum Strain and Tsai-Wu first-ply failure criteria. The variation of failure indices with loading duration and loading magnitude are

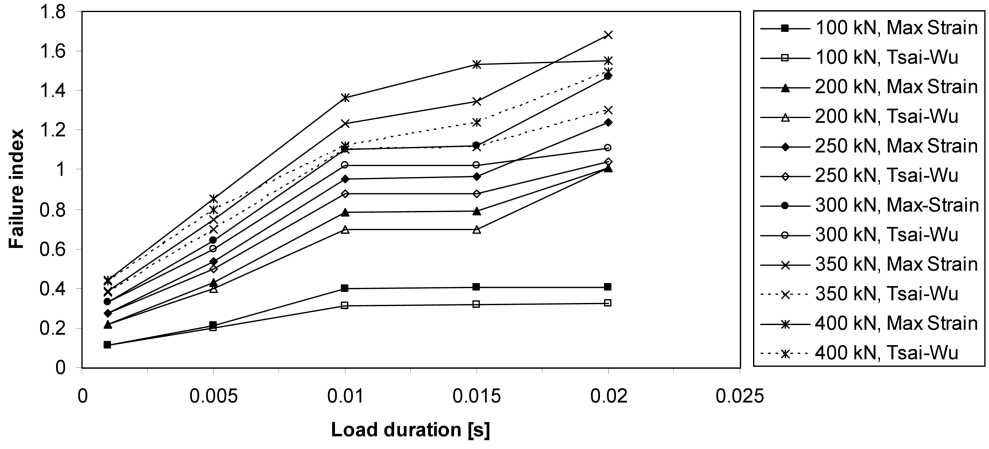

Fig. 17 Variation of failure index with loading duration for Maximum Strain and Tsai-Wu criteria

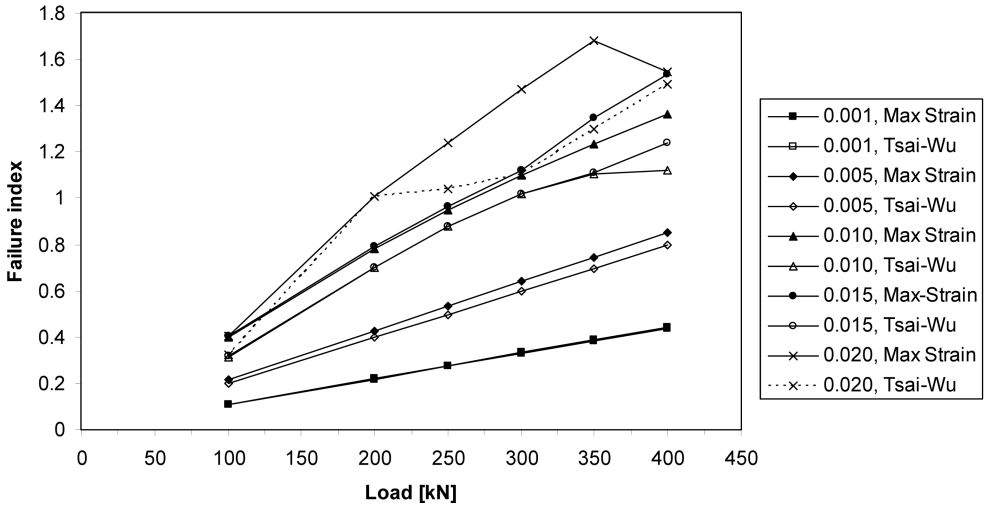

Fig. 18 Variation of failure index with load magnitude for Maximum Strain and Tsai-Wu criteria

reported in Figs. 17 and 18, respectively. It can be observed that, when the loading duration and magnitude are increasing, the failure indices are also increasing.

4.4 Dynamic buckling load

The variation of the dynamic buckling load with the load duration is shown in Fig. 19 along with the static buckling load. In particular, two curves are reported for the dynamic buckling loads: the first one taking as reference for the definition of the dynamic buckling the axial shortening, and the second one taking as reference the radial displacement.

It can be observed that, when the load duration is very short, the dynamic buckling load is higher than the static buckling load, while, when the duration increases, the dynamic buckling load decreases and become lower than the static buckling load.

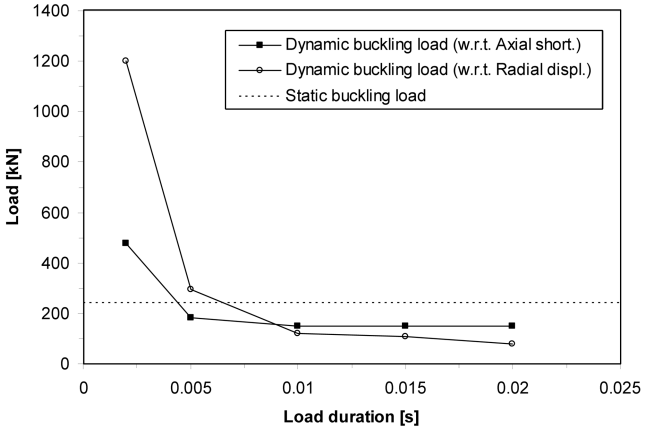

Fig. 19 Variation of buckling loads with load durations

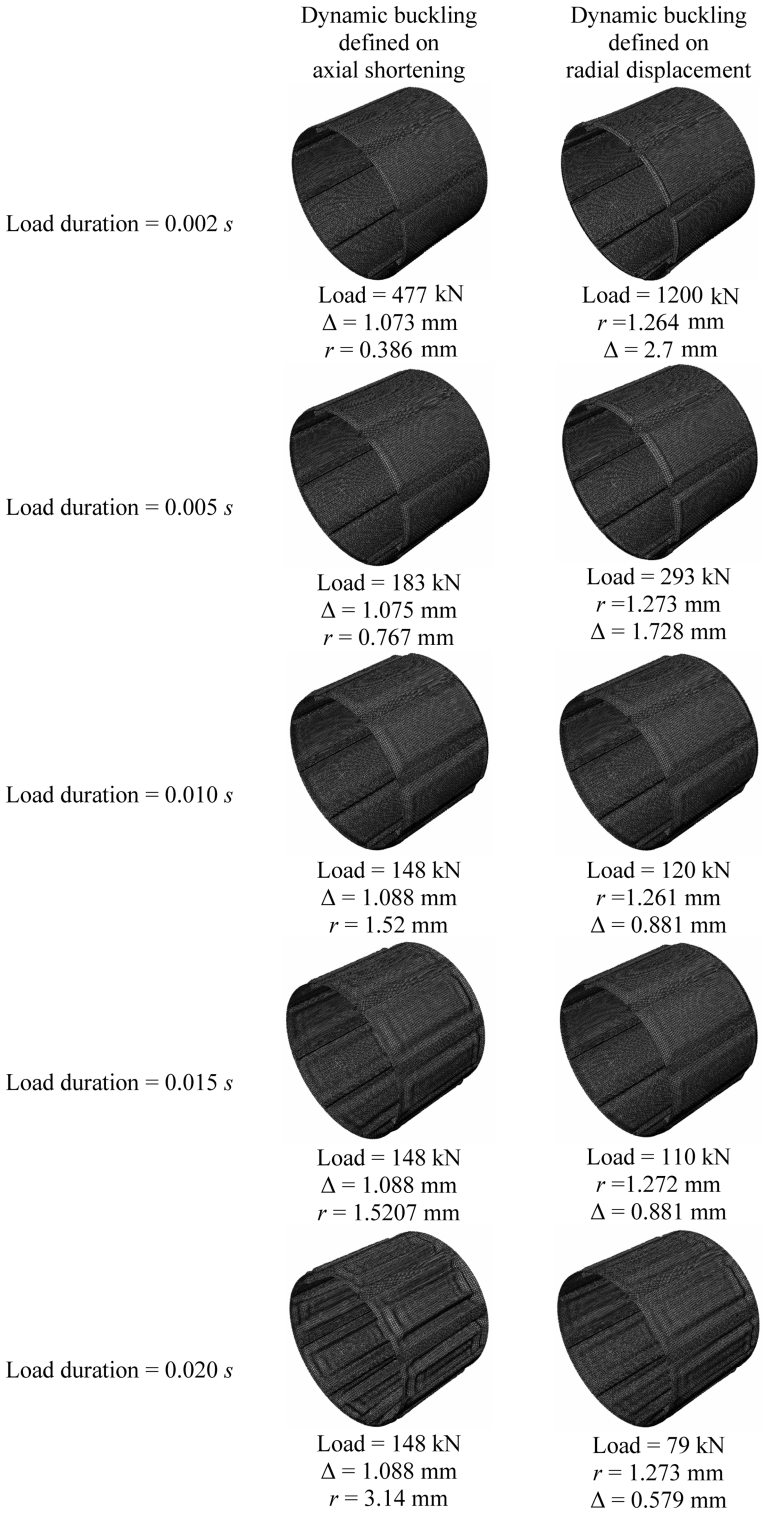

Fig. 20 Dynamic deformation for different load durations

These results, already observed in literature (Huyan and Simitses 1997, Bisagni 2005), show how sensitive is the dynamic buckling load to the load duration. Consequently, if a structure is designed for the static buckling load, it results safe for the dynamic loads only for short duration.

The deformations obtained during the dynamic buckling analyses are shown in Fig. 20. In correspondence to the different analysed load durations, two deformations of the cylindrical stiffened shells are reported: the first one taken when the axial shortening reaches the critical value equal to 1.07 mm, and the second one taken when the radial displacement reaches the critical value equal to 1.26 mm.

For each buckling deformation the Fig. 20 reports also the load magnitude as well as the value of axial shortening Δ and radial displacement r.

It can be observed from the Fig. 19 that, in the case of short load duration, less load is required for the axial shortening to reach the buckling value, while higher load is required for the radial displacement to reach the buckling value. On the other hand this behaviour is opposite for the long load duration.

The dynamic buckling mode, as the static one, is a local buckling phenomenon for the given structure.

The failure indices are high, close to 1.0, at the dynamic buckling load for short duration, while they decrease and become much lower then 1.0 at the dynamic critical loads with long duration. Also the failure area changes with the load duration. In particular, according to the Maximum Strain theory, it is in the top portion of the skin for short duration, and it is at the bottom portion of the skin for longer duration. According to Tsai-Wu criteria the failure area changes in the same way from top to bottom with the increase of the load duration, but it involves both the skin and the stiffeners.

5. Conclusions

The paper investigates the dynamic buckling behaviour of a laminated composite stiffened cylindrical shell using the commercial finite element code ABAQUS.

The numerical model of the composite shell is validated by static tests. In particular, the experimental collapse test is numerically simulated by a quasi static analysis carried out by both ABAQUS/Standard and ABAQUS/Explicit. From these analyses it is found that:

1. The same results are obtained by both types of analyses.
2. The results match well with the experimental data, as collapse load is within 5% variation and the numerical post-buckling deformation is similar to the experimental post-buckling one.
3. The first-ply failure occurs at the point when the load is maximum, that is also named collapse load.
4. The CPU time required by ABAQUS/Standard analysis is, for this simulation, 1.75 times more than that one of the ABAQUS/Explicit analysis.

The validated model of the stiffened composite cylindrical shell is then used to study the dynamic buckling behaviour with ABAQUS/Explicit. The effect of the loading magnitude and of the loading duration are investigated, analyzing both the axial shortening and the radial displacement and implementing first-ply failure criteria. It is observed that the dynamic buckling load is highly affected by the loading duration and magnitude. In particular it is found that:

1. Two definitions of the dynamic buckling load can be considered, taking into account the axial

shortening and the maximum radial displacement, respectively.

2. A small load is required for the axial shortening to reach the buckling value while a large load is required for the radial displacement to reach the buckling value, in the case of short load durations, while this behaviour is opposite for long load durations.

3. The dynamic buckling loads are higher than the static buckling load for short durations, while for long durations the dynamic buckling loads are much lower than the static buckling load.

4. The failure index is high and close to 1.0 at the buckling load for short durations, while it decreases much below 1.0 when the loading duration increases.

All the conclusions regarding the dynamic buckling loads are based on a numerical investigation, and so they need to be validated by experimental tests that are planned for the near future.

Acknowledgements

The first author is grateful to the Italian Ministry of University and Research for providing a "Borsa a favore di giovani ricercatori indiani, A.F. 2007", that has allowed him to perform his post-doc at Politecnico di Milano.

References

Abramovich, H. and Grunwald, A. (1995), "Stability of axially impacted composite plates", *Compos. Struct.*, **32**, 151-158.

Ari-Gur, J. and Simonetta, S.R. (1997), "Dynamic pulse buckling of rectangular composite plates", *Compos. Part B,* **28**, 301-308.

Bisagni, C. (2004), "Dynamic buckling tests of cylindrical shells in composite materials", *Proceedings of the 24th International Congress of the Aeronautical Sciences – ICAS 2004*, Yokohama, August-September.

Bisagni, C. and Cordisco, P. (2004), "Testing of stiffened composite cylindrical shells in the postbuckling range until failure", *AIAA J.*, **42**(9), 1806-1817.

Bisagni, C. (2005), "Dynamic buckling of fiber composite shells under impulsive axial compression", *Thin Wall. Struct.*, **43**, 499-514.

Bisagni, C. and Linde, P. (2006), "Numerical simulation of the structural behaviour of ortothropically stiffened aircraft panels under short time duration loading", *Proceedings of the 25th International Congress of the Aeronautical Sciences - ICAS 2006*, Hamburg, September.

Budiansky, B. and Roth, R.S. (1962), "Axisymmetric dynamic buckling of clamped shallow spherical shells", *Collected Papers on Instability of Shell Structures*, NASA TN-D-1510, 597-606.

Gupta, S.S., Patel, B.P. and Ganapathi, M. (2003), "Nonlinear dynamic buckling of laminated angle-ply composite spherical caps", *Struct. Eng. Mech.*, **15**(4), 463-476.

Huyan, X. and Simitses, G.J. (1997), "Dynamic buckling of imperfect cylindrical shells under axial compression and bending moment", *AIAA J.*, **35**(8), 1404-1412.

Jansen., E.L. (2005), "Dynamic stability problems of anisotropic cylindrical shells via a simplified analysis", *Nonlinear Dynam.*, **39**, 349-367.

Karagiozova, D. and Jones, N. (1996), "Multi-degrees of freedom model for dynamic buckling of an elastic-plastic structure", *Int. J. Solids Struct.*, **33**(23), 3377-3398.

Kolakowski, Z. and Kubiak, T. (2007), "Interactive dynamic buckling of orthotropic thin-walled channels subjected to in-plane pulse loading", *Compos. Struct.*, **81**, 222-232.

Kubiak, T. (2007), "Criteria of dynamic buckling estimation of thin-walled structures", *Thin Wall. Struct.*, **45**, 888-892.

Lindberg, H.E. and Florence, A.L. (1987), *Dynamic Pulse Buckling-theory and Experiment*, Martinus Nijhoff

Publishers, The Netherlands.
Liu, Z.S., Lee, H.P. and Lu, C. (2005), "Numerical study of dynamic buckling for plate and shell structures", *Struct. Eng. Mech.*, **20**(2), 241-257.
Papazoglou, V.J. and Tsouvalis, N.G. (1995), "Large deflection dynamic response of composite laminated plates under in-plane loads", *Compos. Struct.*, **33**, 237-252.
Petry, D. and Fahlbusch, G. (2000), "Dynamic buckling of thin isotropic plates subjected to in-plane impact", *Thin Wall. Struct.*, **38**, 267-283.
Simitses, G.J. (1990), *Dynamic Stability of Suddenly Loaded Structures*, Springers.
Sofiyev, A.H. (2005), "The torsional buckling analysis for cylindrical shell with material non-homogeneity in thickness direction under impulsive loading", *Struct. Eng. Mech.*, **19**(2), 231-236.
Volmir, S.A. (1972), *Nonlinear Dynamics of Plates and Shells*, Science, Moscow.
Yaffe, R. and Abramovich, H. (2003), "Dynamic buckling of cylindrical stringer stiffened shells", *Comput. Struct.*, **81**, 1031-1039.